

WEIGHING THE GALACTIC DARK MATTER HALO: A LOWER MASS LIMIT FROM THE FASTEST HALO STAR KNOWN

NORBERT PRZYBILLA, ALFRED TILICH AND ULRICH HEBER

Dr. Karl Remeis-Observatory Bamberg & ECAP, University Erlangen-Nuremberg, Sternwartstr. 7, D-96049 Bamberg, Germany

AND

RALF-DIETER SCHOLZ

Astrophysikalisches Institut Potsdam, An der Sternwarte 16, D-14482 Potsdam, Germany

Draft version March 8, 2018

ABSTRACT

The mass of the Galactic dark matter halo is under vivid discussion. A recent study by Xue et al. (2008, ApJ, 684, 1143) revised the Galactic halo mass downward by a factor of ~ 2 relative to previous work, based on the line-of-sight velocity distribution of ~ 2400 blue horizontal-branch (BHB) halo stars. The observations were interpreted in a statistical approach using cosmological galaxy formation simulations, as only four of the 6D phase-space coordinates were determined. Here we concentrate on a close investigation of the stars with highest negative radial velocity from that sample. For one star, SDSSJ153935.67+023909.8 (J1539+0239 for short), we succeed in measuring a significant proper motion, i.e. full phase-space information is obtained. We confirm the star to be a Population II BHB star from an independent quantitative analysis of the SDSS spectrum – providing the first NLTE study of any halo BHB star – and reconstruct its 3D trajectory in the Galactic potential. J1539+0239 turns out as the fastest halo star known to date, with a Galactic rest-frame velocity of 694^{+300}_{-221} km s⁻¹ (full uncertainty range from Monte Carlo error propagation) at its current position. The extreme kinematics of the star allows a significant lower limit to be put on the halo mass in order to keep it bound, of $M_{\text{halo}} \geq 1.7^{+2.3}_{-1.1} \times 10^{12} M_{\odot}$. We conclude that the Xue et al. results tend to underestimate the true halo mass as their most likely mass value is consistent with our analysis only at a level of 4%. However, our result confirms other studies that make use of the full phase-space information.

Subject headings: dark matter — Galaxy: halo — stars: atmospheres — stars: horizontal-branch — stars: kinematics and dynamics — stars: Population II

1. INTRODUCTION

Knowledge of the properties of dark matter halos is an important issue for our understanding of galaxy formation and evolution, and for unveiling the nature of dark matter. The halo of the Milky Way therefore is of highest interest, as it allows unique observational constraints to be obtained for testing theoretical models (e.g. Navarro et al. 1996). Several observational campaigns – e.g. the Sloan Digital Sky Survey (SDSS, York et al. 2000), the Radial Velocity Experiment (RAVE, Steinmetz et al. 2006), the Sloan Extension for Galactic Understanding and Exploration (SEGUE, Yanny et al. 2009) – provide the tracers for studying halo properties, like the total mass of the halo and its extent.

Several studies in the past decade determined the halo mass from ever increasing samples of halo stars, globular clusters and/or satellite galaxies. However, it is in fact only a few objects at highest velocity that are affecting largely the mass estimates (Sakamoto et al. 2003; Smith et al. 2007). While larger halo masses of about $2 \times 10^{12} M_{\odot}$ were favoured earlier (Wilkinson & Evans 1999; Sakamoto et al. 2003), lower masses of about half this value were derived more recently (Battaglia et al. 2005; Smith et al. 2007; Xue et al. 2008). The precise value determines, e.g. among others, whether satellite galaxies like the Magellanic Clouds (e.g. Kallivayalil et al. 2006; Costa et al. 2009) or hyper-velocity star¹ candidates

(Abadi et al. 2009) are on bound orbits, or not.

Most of the previous studies had to rely substantially on the *distributions* of radial velocities in their samples to derive their conclusions as full space motions for halo objects are unavailable in many cases at present. In such cases only four coordinates (i.e. two position values, distance and radial velocity, RV) of the 6D phase space are determined and the missing data (the proper motion components) are handled in a statistical approach. E.g., radial velocities for more than 10,000 blue halo stars from the SDSS were measured in the yet most extensive study by Xue et al. (2008). The sample was composed of blue horizontal-branch, blue straggler, and main-sequence stars with effective temperatures roughly between 7,000 and 10,000 K according to their colours. Here, we focus on the fastest stars of the Xue et al. sample in terms of *negative* line-of-sight velocity, indicating a *bound* orbit.

For one of them we were able to measure a significant proper motion, which allowed a detailed 3D kinematic investigation when combined with a quantitative spectroscopic analysis that facilitated the determination of the star's distance. SDSSJ153935.67+023909.8 (J1539+0239 for short) is an inbound² Population II horizontal branch star with a

with the super-massive black hole (Hills 1988).

² An extragalactic origin of the star as an unbound low-mass hyper-velocity star from another galaxy is imaginable but unlikely. The local volume is devoid of galaxies in a wide range (several 10 deg) around the infall direction of J1539+0239 at present (for the Local Group see van den Bergh 1999, and later discoveries). If ejected early after its formation, the star could have travelled ~ 8 Mpc during its lifetime, such that a final answer on this may be only obtained when full space motions of the nearby galaxies are known.

Norbert.Przybilla@sternwarte.uni-erlangen.de

¹ Hyper-velocity stars move at such high velocity that they may be gravitationally unbound to the Galaxy. Their supposed place of origin is the Galactic center, where they may have been accelerated by gravitational interactions

Galactic rest-frame (GRF) velocity of $\sim 700 \text{ km s}^{-1}$ at its current position, making it the fastest halo object known. This allows a significant lower limit for the total halo mass of the Galaxy to be set. The present work provides a glimpse to the detailed kinematic investigations feasible once the European Space Agency’s Gaia satellite mission (e.g. Turon et al. 2005) becomes operational, at much higher precision.

2. TARGET SELECTION AND PROPER MOTION

In a previous paper (Tillich et al. 2009) we already investigated the high-velocity tail of the Xue et al. (2008) sample and found a hyper-velocity candidate of spectral type A among the stars with highest *positive* radial velocities in the GRF. Here we study the most extreme stars approaching us, applying the same techniques. We selected all stars with GRF velocities $v_{\text{GRF}} < -350 \text{ km s}^{-1}$ from the RV-based sample of Xue et al. (2008) and obtained 5 targets for which we attempted to measure proper motions. All available independent position measurements on Schmidt plates (APM - McMahon et al. (2000); SSS - Hambly et al. (2001)) were collected and combined with the *SDSS* and other available positions (CMC14 Carlsberg-Meridian-Catalog (2006); 2MASS - Cutri et al. (2003); UKIDSS - Lawrence et al. (2007)) for a first linear proper motion fit. However, there were even more measurements of Schmidt plates, from up to 14 different epochs in case of overlapping plates of the Digitised Sky Surveys³. FITS images of 15 by 15 arcmin size were extracted from all available plates and ESO MIDAS tools were used to measure positions. For this purpose, we selected compact background galaxies around each target, identified from *SDSS*, to transform the target positions on all the Schmidt plates to the *SDSS* system. The small fields allowed us to apply a simple model (shift+rotation) and to achieve a higher accuracy in our final proper motion fit for all our targets (see e.g. Fig. 1). We consider a positive detection if the proper motion errors σ of both components are below 3.0 mas yr^{-1} and if at least one of the components is significant (above 3σ). For J1539+0239, the brightest of our five targets, we found a highly significant proper motion of $\mu_{\alpha} \cos \delta = -10.6 \pm 1.6 \text{ mas yr}^{-1}$ and $\mu_{\delta} = -10.0 \pm 2.3 \text{ mas yr}^{-1}$, whereas for the other four fainter stars (with *V* magnitudes between 17 and 20) the proper motion was consistent with zero. The proper motions as well as their transformations from equatorial to Galactic coordinates are summarized in Table 1.

3. OBSERVATIONS AND QUANTITATIVE SPECTROSCOPY

In order to exclude RV variability, we re-observed J1539+0239 with the TWIN spectrograph at the 3.5m telescope on Calar Alto in May 2009. Radial velocities were derived by χ^2 -fitting of adequate synthetic spectra over the full spectral range, yielding a heliocentric radial velocity of $v_{\text{rad}} = -366.6 \pm 4.0 \text{ km s}^{-1}$ for the TWIN spectrum, which is consistent with the $v_{\text{rad}} = -372.6 \pm 5.8 \text{ km s}^{-1}$ measured from the *SDSS* data within the mutual uncertainties. We use the latter value for the kinematic study.

A quantitative analysis of J1539+0239 was carried out following the hybrid NLTE approach discussed by Przybilla et al. (2006). In brief, line-blanketed LTE model atmospheres were computed with ATLAS9 (Kurucz 1993) and NLTE (and LTE) line-formation calculations were performed using updated versions of DETAIL and SURFACE (Giddings

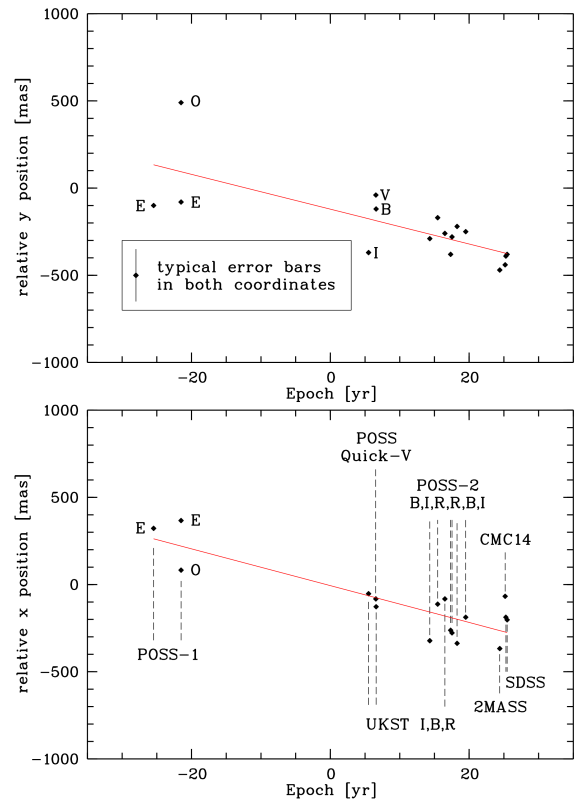


Fig. 1.— Linear fit of the position measurements for J1539+0239 with a zero epoch of 1975.39.

1981; Butler & Giddings 1985). Many astrophysically important chemical species were treated in NLTE, using state-of-the-art model atoms (H: Przybilla & Butler 2004a; C I: Przybilla et al. 2001b; N I: Przybilla & Butler 2001; O I: Przybilla et al. 2000; Mg I/II: Przybilla et al. 2001a; Ti II and Fe II: Becker 1998).

The effective temperature T_{eff} and the surface gravity $\log g$ were determined by fits to the Stark-broadened Balmer and Paschen lines and an ionization equilibrium, here of Mg I/II, in analogy to previous work on hyper-velocity stars at similar temperatures (Przybilla et al. 2008; Tillich et al. 2009). The stellar metallicity was derived by model fits to the observed metal line spectra. Results are listed in Table 1 and a comparison of the resulting final synthetic spectrum with observation is shown in Fig. 2. Overall, excellent agreement is obtained for the strategic spectral lines throughout the entire wavelength range. Our stellar parameters ($T_{\text{eff}} = 7700 \pm 250 \text{ K}$, $\log g = 3.00 \pm 0.15$) are consistent with those derived in the LTE analysis by Xue et al. (2008): $T_{\text{eff}} = 7807 \text{ K}$, $\log g = 3.16$. We constrained the errors in the stellar parameters by the quality of the match of the spectral indicators within the given S/N limitations.

Its parameters place J1539+0239 on the horizontal branch at a mass of $0.68 \pm 0.05 M_{\odot}$ as derived by comparing the position of the star in the $T_{\text{eff}}\text{-}\log g$ -diagram to predictions of the evolutionary models of Dorman et al. (1993). No rotational broadening was detected at the resolution of the *SDSS* spectrum. The metallicity is lower than solar by a factor of 100 and the abundances of the α -elements are enhanced by about

³ http://archive.stsci.edu/cgi-bin/dss_plate_finder

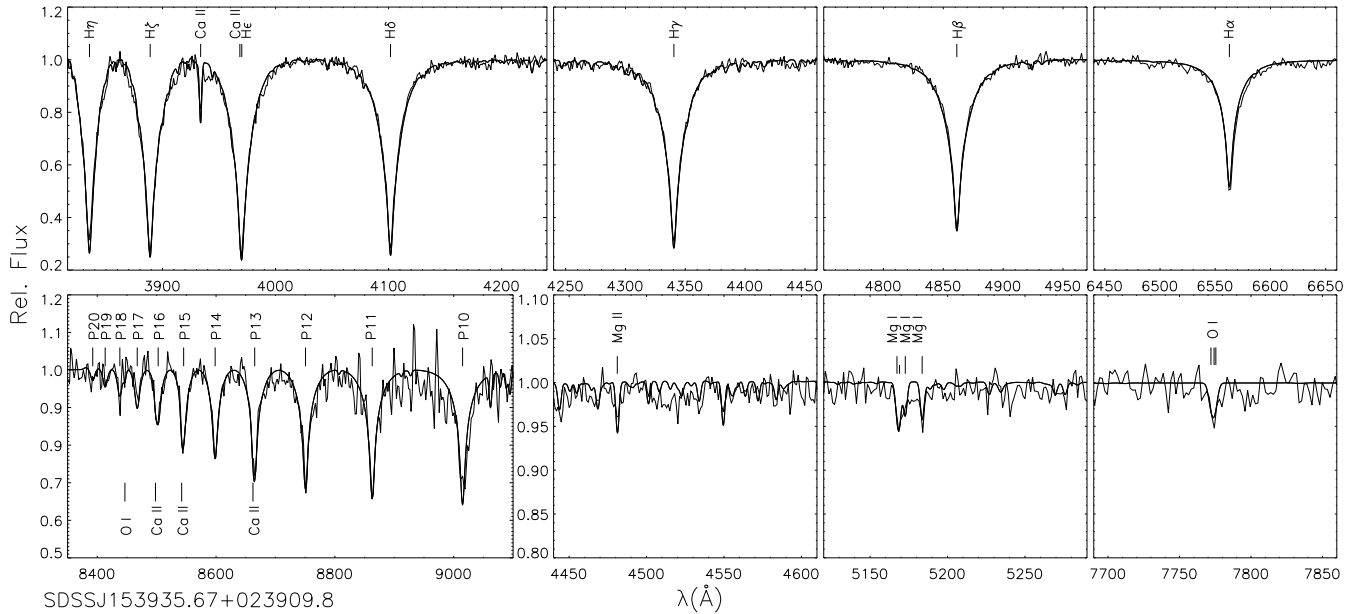


Fig. 2.— Comparison of NLTE spectrum synthesis (thick line) with observation (*SDSS*, thin wiggly line) for J1539+0239. Displayed are selected regions around the Balmer lines, the higher Paschen series, Mg II $\lambda 4481\text{\AA}$, the Mg I b and the near-IR O I triplets.

TABLE 1
RESULTS OF THE SPECTROSCOPIC AND KINEMATIC ANALYSIS OF J1539+0239.

| | | | |
|--|------------------|--|---------------------|
| V (mag) ^a | 15.72 ± 0.02 | $E(B - V)$ (mag) ^b | 0.04 ± 0.03 |
| $\mu_{\alpha} \cos \delta$ (mas yr ⁻¹) | -10.6 ± 1.6 | μ_{δ} (mas yr ⁻¹) | -10.0 ± 2.3 |
| l (deg) | 8.9836 | b (deg) | +42.9515 |
| $\mu_l \cos b$ (mas yr ⁻¹) | -14.3 ± 2.1 | μ_b (mas yr ⁻¹) | $+2.8 \pm 1.9$ |
| T_{eff} (K) | 7700 ± 250 | $\log g$ (cgs) | 3.00 ± 0.15 |
| $[M/H]$ | -2.0α | $[\alpha/Fe]$ | +0.4 |
| M/M_{\odot} | 0.68 ± 0.05 | d (kpc) | 12.0 ± 2.3 |
| v_{rad} (km s ⁻¹) | -372.6 ± 5.8 | v_{GRF} (km s ⁻¹) | 694^{+300}_{-221} |
| v_{esc} (km s ⁻¹) | 519 | | |

^a The visual magnitude has been derived from *SDSS* magnitudes following Jordi et al. (2006)

^b The interstellar colour excess $E(B-V)$ has been determined by comparing the observed colours to synthetic ones from the model spectral energy distribution.

0.4 dex with respect to iron, which is typical for the halo population. We conclude that the star is a horizontal branch star of Population II. All results are summarised in Table 1.

Before proceeding to the further discussion it may be instructive to take a closer look on the spectrum synthesis in NLTE and LTE, as this has not been done for Population II blue horizontal branch-stars so far. A few comparisons of NLTE and LTE profiles are therefore shown in Fig. 3. The combination of a higher T_{eff} than typically found for Population II stars and the diminished line blocking because of the low metal content results in a hardened radiation field which, along with reduced thermalizing effects because of smaller collision rates in the low-density atmosphere, leads to pronounced NLTE effects on many diagnostic lines. NLTE strengthening is found for the Doppler core of $H\alpha$ – in line with the behaviour in cool stars (e.g. Przybilla & Butler 2004b) –, while the inner line wings are weakened. The higher Balmer and Paschen lines show much lower deviations from LTE. Our calculations predict the majority of the weak

lines to be described well by the assumption of LTE. On the other hand, many of the stronger metal lines, as e.g. of C I, O I, Mg I/II or Fe II – the diagnostic lines at the spectroscopic resolution achieved within the *SDSS* – show pronounced NLTE strengthening. In order to reproduce the NLTE equivalent widths of these particular lines, abundance corrections need to be applied of about 0.1 dex (Mg II), 0.2 dex (Mg I, Fe II), 0.5 dex (O I) and 1.9 dex (C I) in LTE. Note, however, that these line are close to saturation. LTE computations with increased abundances can therefore not reproduce the NLTE line depths at all, instead stronger line wings develop. Abundance studies based on equivalent widths may therefore be misleading, as such differences remain unnoticed. An investigation at high spectral resolution would therefore be worthwhile in order to facilitate the NLTE effects to be studied in detail.

4. DISTANCE, KINEMATICS AND ERRORS

Using the mass, effective temperature, gravity and extinction-corrected apparent magnitude we derive the distance following Ramspeck et al. (2001) using the fluxes from the final model spectrum in analogy to previous work (Tillich et al. 2009). The distance error is dominated by the gravity error.

Applying the Galactic potential of Allen & Santillan (1991) we calculated orbits and reconstructed the path of the star through the Galactic halo with the program of Odenkirchen & Brosche (1992). The distance of the Galactic center from the Sun was adopted to be 8.0 kpc and the Sun’s motion with respect to the local standard of rest was taken from Dehnen & Binney (1998). As the RV is well known the error of the space motion is dominated by that of the distance, ruled by the gravity error, and those of the proper motion components. Varying these three quantities within their respective errors we applied a Monte-Carlo procedure to derive the median GRF velocity v_{GRF} at the present location and the velocity distribution (see Fig. 4) and compare with the local escape velocity v_{esc} as calculated from the Galactic potential

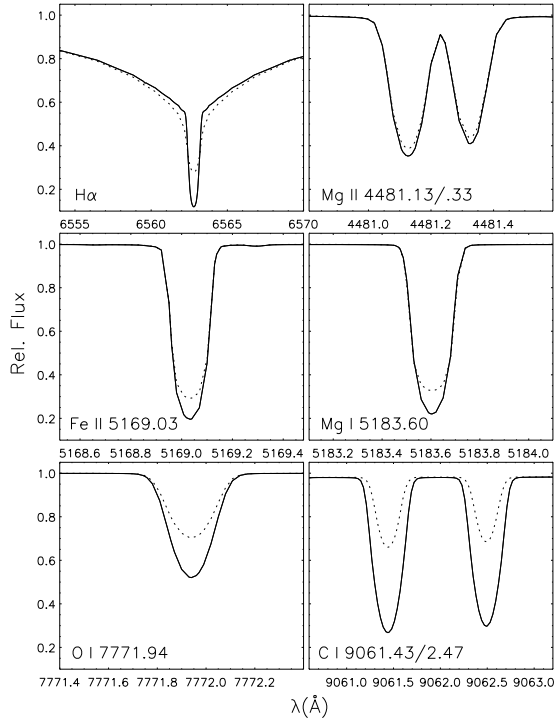


FIG. 3.— Comparison of NLTE (full lines) and LTE (dotted) line profiles from calculations for our adopted model parameters for J1539+0239. Displayed are examples of strong lines that can be used for diagnostics at the *SDSS* spectral resolution.

of Allen & Santillan (1991).

A median GRF velocity of 694 km s^{-1} (with the velocity distribution ranging from -221 to $+300 \text{ km s}^{-1}$ around this value) makes J1539+0239 the fastest halo star known, superseding CS 22183–0014 (at $v_{\text{GRF}} = 635 \pm 127 \text{ km s}^{-1}$, Sakamoto et al. 2003). This value is above the local escape velocity of $v_{\text{esc}} \approx 519 \text{ km s}^{-1}$ in the potential of Allen & Santillan (1991). This three component potential consists of a central bulge and a disk, which have a combined mass of $M_{\text{bulge+disk}} \approx 10^{11} M_{\odot}$. The halo out to 100 kpc is assumed to have a total mass of $M_{\text{halo}} \approx 8 \times 10^{11} M_{\odot}$. This total halo mass is insufficient to keep the star bound to the Galaxy.

J1539+0239 is located in the northern Galactic hemisphere ($l \approx 9.0$, $b \approx 42.95$), in the direction close to the Sagittarius stream (Belokurov et al. 2006; Fellhauer et al. 2006) and in particular close to the globular clusters NGC 5904 and Palomar 5, with its tidal tail (Odenkirchen et al. 2003). However, it is unlikely that J1539+0239 is related to either of those because of its distinct space motion and its position in the foreground. Its position and kinematics also rule out a scenario of a *recent* acceleration by an interaction with the super-massive black hole in the Galactic center, the principal mechanism for generating hyper-velocity stars (Hills 1988). The star is currently *approaching* the Galactic disk and will pass the Galactic center at a minimum distance of about 8 kpc in the future. See Fig. 5 for a visualization of the orbit of J1539+0239 in the Galactic halo (upper panel) and a for a magnification of the Galactic disk region of the trajectory (lower panel).

Hence, in order to keep the trajectory of J1539+0239 bound to the Galaxy, the dark matter halo mass needs to be adjusted. We carried out numerical experiments increasing the

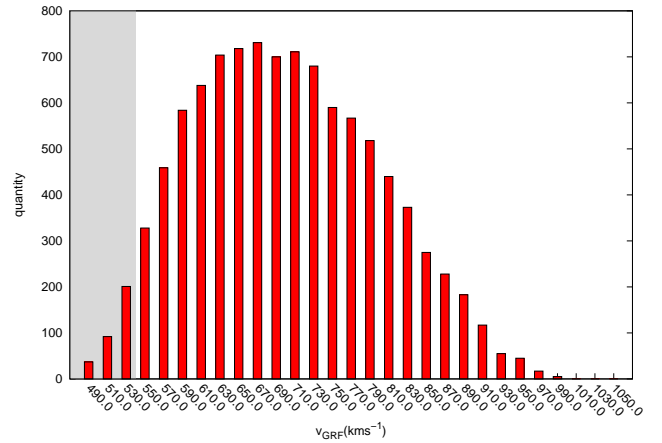


FIG. 4.— Galactic restframe velocity distribution for J1539+0239 derived from a Monte Carlo procedure with a depth of 10,000. The grey shaded area indicates the fraction of trajectories that would be bound for $M_{\text{halo}} = 1.0 \times 10^{12} M_{\odot}$, the most likely halo mass of Xue et al. (2008).

halo density by a constant factor. Finally we found a bound trajectory for a minimum mass of $M_{\text{halo}}^{\text{new}} = 1.7 \times 10^{12} M_{\odot}$. The last pericenter passage occurred at a distance of ~ 7.7 kpc and the apocenter distance of the star’s trajectory is located far out in the halo, at ~ 250 kpc in this case. If we take into account the full velocity distribution (see Fig. 4) of the star we even can derive solutions for the extrema, which correspond to the absolute errors, giving $M_{\text{halo}} \sim 1.7^{+2.3}_{-1.1} \times 10^{12} M_{\odot}$.

Whether the star is bound to the Galaxy highly depends on the Galactic potential adopted, in particular on the mass of the dark matter halo, as pointed out by Abadi et al. (2009). Our M_{halo} is similar to values found in several recent studies. Wilkinson & Evans (1999) used 27 satellite galaxies and globular clusters, by assuming that they are bound and derived a total Galactic halo mass of $M_{\text{halo}} \sim 1.9^{+3.6}_{-1.7} \times 10^{12} M_{\odot}$. This value matches our derivation but has a larger uncertainty. Sakamoto et al. (2003) used 11 satellite galaxies, 137 globular clusters and 413 field horizontal branch stars to derive a total Galactic mass. The exclusion of Leo I from their sample would lower the total Galactic mass from $M_{\text{total}} \sim 2.5^{+0.5}_{-1.0} \times 10^{12} M_{\odot}$ to a value of $M_{\text{total}} \sim 1.8^{+0.4}_{-0.7} \times 10^{12} M_{\odot}$, both again in excellent agreement with our finding.

On the other hand, less than 4% of the trajectories resulting from our MC simulations would be bound for the most likely mass of Xue et al., $M_{\text{halo}} = 1.0 \times 10^{12} M_{\odot}$ (grey shaded area in Fig. 4). Their RV study of ~ 2400 blue horizontal-branch stars – which includes J1539+0239 but lacks any proper motion measurements – therefore likely underestimate the Galactic halo mass.

5. SUMMARY AND CONCLUSIONS

We reported the quantitative spectral analysis of a high-velocity star from the sample of faint blue halo stars of Xue et al. (2008). J1539+0239 was confirmed to be a Population II blue horizontal branch star with a low metallicity of $[\text{Fe}/\text{H}] = -2.0$ and the characteristic enhancement of α -elements. Hereby, we performed a NLTE analysis of a halo BHB star for the first time. While the majority of the weak lines were confirmed to be formed close to LTE conditions, many of the stronger metal lines – which are important diagnostics at the spectral resolution achieved within the *SDSS* – show pronounced NLTE strengthening, with the differences

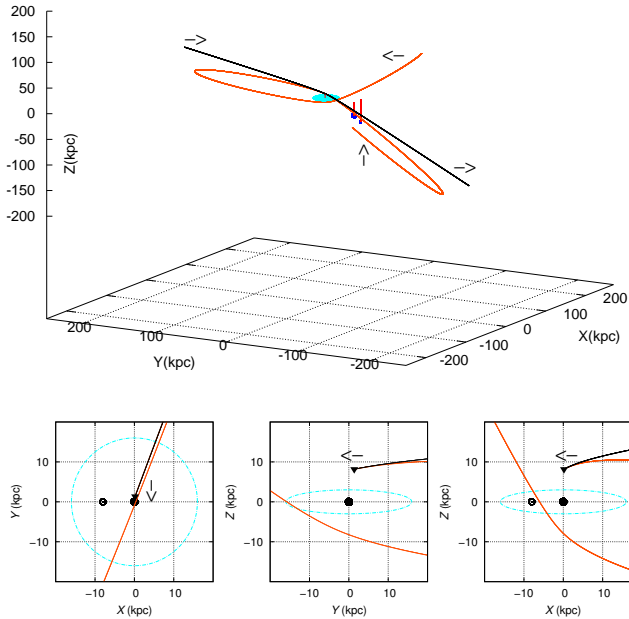


Fig. 5.— Upper panel: Trajectories for the metal-poor horizontal branch star J1539+0239, relatively to the Galactic disk (light blue). Applying a standard potential (Allen & Santillan 1991) the trajectory is unbound (black, $t \approx \pm 0.5$ Gyr), while increasing the halo density we found a bound trajectory (red, $-3 \text{ Gyr} \leq t \leq +2 \text{ Gyr}$). For reference, the Magellanic Clouds (blue dots) and the current position of J1539+0239 (black triangle) are marked. Lower panel: schematic 2D-visualization of the central region. Details of the trajectory in the immediate past and around the previous pericenter passage of J1539+0239 (bound solution) are shown in the X - Y , Y - Z and X - Z planes. The positions of the Galactic center (black dot) and of the Sun are indicated.

between the derived LTE and NLTE abundances amounting to 0.1 dex to 0.5 dex typically. In addition to information on the chemical composition, the radial velocity, proper motion and spectroscopic distance were derived and a detailed kinematical analysis was performed.

Carrying out kinematical numerical experiments using the Galactic potential of Allen & Santillan (1991) in order to obtain an orbit of J1539+0239 gravitationally bound to the Milky Way, we found that the mass of the dark halo has to be at least $M_{\text{halo}} \sim 1.7^{+2.3}_{-1.1} \times 10^{12} M_{\odot}$ (absolute uncertainties from extrema in MC error propagation). This mass limit is in good agreement with several previous studies (Wilkinson & Evans 1999; Sakamoto et al. 2003; Abadi et al. 2009). However, the significantly lower most likely mass value of Xue et al. (2008) is consistent with our analysis only at a level of 4%, i.e. it likely underestimates the Galactic dark halo mass.

We conclude, that if the kinematics of a halo star is extraordinary enough, and the errors within the analysis are small, even *one* star alone can provide a significant lower limit to the dark matter halo mass, and to the total mass of the Milky Way (halo + bulge + disk), here $M_{\text{total}} \geq 1.8^{+2.3}_{-1.1} \times 10^{12} M_{\odot}$. The determining factor is that full kinematic information is available, as it will become routine in the era of the Gaia space mission, at much higher precision.

A.T. acknowledges funding by the Deutsche Forschungsgemeinschaft (DFG) through grant HE1356/45-1. Travel to the DSAZ (Calar Alto, Spain) was supported by the DFG under grant HE1356/50-1. We are very grateful to Stephan Geier for stimulating discussions and advice. Our thanks go to S. Müller and T. Kupfer for observing and reducing the data from DSAZ. Funding for the SDSS and SDSS-II has been provided by the Alfred P. Sloan Foundation, the Participating Institutions, the National Science Foundation, the U.S. Department of Energy, the National Aeronautics and Space Administration, the Japanese Monbukagakusho, the Max Planck Society, and the Higher Education Funding Council for England. The SDSS Web Site is <http://www.sdss.org/>.

Facilities: Sloan, CAO:3.5m (TWIN).

REFERENCES

- Abadi, M. G., Navarro, J. F., & Steinmetz, M. 2009, *ApJ*, 691, L63
 Allen, C. & Santillan, A. 1991, *Rev. Mex. Astr. Astrofis.*, 22, 255
 Battaglia, G., Helmi, A., Morrison, H., et al. 2005, *MNRAS*, 364, 433
 Becker, S. R. 1998, in *ASP Conf. Ser.*, Vol. 131, Boulder-Munich II: Properties of Hot, Luminous Stars, ed. I. Howarth (San Francisco, CA: ASP), 137
 Belokurov, V., Zucker, D. B., Evans, N. W., et al. 2006, *ApJ*, 642, L137
 Butler, K., & Giddings, J. R. 1985, in *Newsletter of Analysis of Astronomical Spectra*, No. 9 (London: Univ. London)
 Carlsberg-Meridian-Catalog. 2006, Copenhagen Univ. Obs., Inst. of Astr., Cambridge, UK, Real Inst. y Obs. de la Armada en San Fernando, 1304, 0
 Costa, E., Méndez, R. A., Pedreros, M. H., et al. 2009, *AJ*, 137, 4339
 Cutri, R. M., Skrutskie, M. F., van Dyk, S., et al. 2003, *2MASS All Sky Catalog of point sources*.
 Dehnen, W. & Binney, J. J. 1998, *MNRAS*, 298, 387
 Dorman, B., Rood, R. T., & O’Connell, R. W. 1993, *ApJ*, 419, 596
 Fellhauer, M., Belokurov, V., Evans, N. W., et al. 2006, *ApJ*, 651, 167
 Giddings, J. R. 1981, PhD thesis, Univ. London
 Hambly, N. C., MacGillivray, H. T., Read, M. A., et al. 2001, *MNRAS*, 326, 1279
 Hills, J.G. 1988, *Nature*, 331, 687
 Jordi, K., Grebel, E. K., & Ammon, K. 2006, *A&A*, 460, 339
 Kallivayalil, N., van der Marel, R. P., & Alcock, C. 2006, *ApJ*, 652, 1213
 Kurucz, R. 1993, Kurucz CD-ROM No. 13 (Cambridge, MA: SAO)
 Lawrence, A., Warren, S. J., Almaini, O., et al. 2007, *MNRAS*, 379, 1599
 McMahon, R. G., Irwin, M. J., & Maddox, S. J. 2000, *VizieR Online Data Catalog*, 1267, 0
 Navarro, J. F., Frenk, C. S., & White, S. D. M. 1996, *ApJ*, 462, 563
 Odenkirchen, M. & Brosche, P. 1992, *Astronomische Nachrichten*, 313, 69
 Odenkirchen, M., Grebel, E. K., Dehnen, W., et al. 2003, *AJ*, 126, 2385
 Przybilla, N., & Butler, K. 2001, *A&A*, 379, 955
 Przybilla, N., & Butler, K. 2004a, *ApJ*, 609, 1181
 Przybilla, N., & Butler, K. 2004b, *ApJ*, 610, L61
 Przybilla, N., Butler, K., Becker, S. R., Kudritzki, R. P., Venn, K. A. 2000, *A&A*, 359, 1085
 Przybilla, N., Butler, K., Becker, S. R., & Kudritzki, R. P. 2001a, *A&A*, 369, 1009
 Przybilla, N., Butler, K., & Kudritzki, R. P. 2001b, *A&A*, 379, 936
 Przybilla, N., Butler, K., Becker, S. R., & Kudritzki, R. P. 2006, *A&A*, 445, 1099
 Przybilla, N., Nieva, M. F., Tillich, A., et al. 2008, *A&A*, 488, L51
 Ramspeck, M., Heber, U., & Moehler, S. 2001, *A&A*, 378, 907
 Sakamoto, T., Chiba, M., & Beers, T. C. 2003, *A&A*, 397, 899
 Smith, M. C., Ruchti, G. R., Helmi, A., et al. 2007, *MNRAS*, 379, 755
 Steinmetz, M., Zwitter, T., Siebert, A., et al. 2006, *AJ*, 132, 1645
 Tillich, A., Przybilla, N., Scholz, R., & Heber, U. 2009, *A&A*, 507, L37
 Turon, C., O’Flaherty, K. S., & Perryman, M. A. C., eds. 2005, *ESA Special Publication*, Vol. 576, *The Three-Dimensional Universe with Gaia van den Bergh, S.* 1999, *A&A Rev.*, 9, 273
 Wilkinson, M. I. & Evans, N. W. 1999, *MNRAS*, 310, 645
 Xue, X. X., Rix, H. W., Zhao, G., et al. 2008, *ApJ*, 684, 1143
 Yanny, B., Rockosi, C., Newberg, H. J., et al. 2009, *AJ*, 137, 4377
 York, D. G., Adelman, J., Anderson, Jr., J. E., et al. 2000, *AJ*, 120, 1579